Numerical simulation of the flow through metallic foams: multiscale modeling and experimental validation

Hétu, J. -F.; Ilinca, F.; Marcotte, J. -P.; Baril, E.; Lefebvre, L. -P.; Innocentini, M.

Publisher's version / Version de l'éditeur:
https://doi.org/10.1063/1.3453826
Porous Media and its Applications in Science, Engineering and Industry: 3rd International Conference, pp. 287-292, 2010-05-30

Numerical Simulation of the Flow Through Metallic Foams: Multiscale Modeling and Experimental Validation

J.-F. Hétu*, F. Ilinca*, J.-P. Marcotte*, E. Baril*, L.P. Lefebvre* and M.Innocentini†

*National Research Council, 75 de Mortagne, Boucherville, Qc, Canada, J4B 6Y4
†Universidade de Riberao Preto, Av. Costabile Romano, 2201, 14096-900, Riberao Preto, SP, Brasil

Abstract. In this work the incompressible steady-state flow through a metallic foam matrix is solved by a finite element method. A multiscale approach combining the solution at the pore level by an immersed boundary method and the macro-scale solution with simulated permeability is used. The micro scale solution of the flow takes into account the details characterizing the geometry of the foam (μCT scans) and is used to determine the permeability coefficients in the Forchheimer's model. In a second step, a numerical approach is used to solve the flow at the macro scale by modelling the presence of the foam via a source term corresponding to the pressure drop computed at the micro scale. Such simulation gives the opportunity to solve the flow in complex configurations in which the foam is only a part of the computational domain. The computed pressure drop as a function of the flow rate on the macro scale configuration replicating an experimental set-up is compared with the experimental data for various foam thicknesses.

Keywords: Metallic foam; Multiscale modeling; Finite elements; Immersed boundary method; Permeability
PACS: 47.11.Fg; 47.11.St; 47.56.+r; 02.60.Cb

INTRODUCTION

Description of the fluid flow through porous medium is important in many industrial applications. This flow is generally described by a parabolic function of the pressure drop in the flow direction as a function of the flow rate (i.e. Forchheimer's equation). Using that equation, the pressure drop can be described knowing the permeability constant (Darcian and Non-Darcian), the viscosity and density of the fluid as well as its velocity. The permeability can be measured experimentally by measuring the pressure drop when the fluid flow through a porous medium at different velocities. The permeability cannot, however, always be easily measured experimentally and new techniques need to be developed. For example, permeability perpendicular to a thin planar medium, such as paper or textile, can be difficult to determine experimentally. Besides, in many applications it is important to describe fluid flow in 3D into complex porous medium to optimize the performance of a devices such as reactors, porous electrodes, catalysts support and filters. Thus, the development of models to describe the flow through porous medium should help developing and optimizing the design of such devices.

The goal of this work is to provide numerical modeling tools for the characterization of the flow through such medium. In this study, the experiments were conducted in metallic foams. Numerical solutions were obtained for various flow regimes and a general relationship between the dimensionless pressure gradient and the Reynolds number was proposed. The numerical solutions were obtained using a multi-scale approach. In a first study, the geometry of the foam was extracted from the volumetric data generated from X-ray micro-CT scans and a level set function was constructed that represents the surface of the metallic structure. The three-dimensional Navier-Stokes equations describing the fluid flow inside the metallic foam was solved on simple quasi-structured meshes of tetrahedrons using a finite element immersed boundary method. In a second step the flow at the macro scale,(in this case the scale of the experimental apparatus), was solved numerically by modeling the presence of the foam though a source term providing the same pressure drop as the one computed on the micro scale. Such simulation gives the opportunity to solve the flow in complex configurations where the porous medium is only a part of the computational domain. The computed pressure drop as a function of the flow rate on the macro scale configuration replicating an experimental setup was then compared with the experimental data for various foam thicknesses. The numerical results for the macro scale simulations confirm several experimental observations: the pressure drop depends on the way the set-up is designed and the pressure drop dependence on the sample thickness decreases as the ratio of the foam section exposed to the flow to the total foam section approaches 1. Simulation results agree very well with the experimental data, thus opening the way for more extensive numerical studies of the flow inside porous media. Such approach could be used for the optimization of the design of new devices involving flow through porous materials.

FLOW MODELING

Model equations and boundary conditions

The equations of motion are the steady-state incompressible Navier-Stokes equations:

$$\rho \mathbf{u} \cdot \nabla \mathbf{u} = -\nabla p + \nabla \cdot \left[\mu \left(\nabla \mathbf{u} + (\nabla \mathbf{u})^T \right) \right] + \mathbf{f} \quad (1)$$

$$\nabla \cdot \mathbf{u} = 0, \quad (2)$$

where ρ is the density, $\mathbf{u}$ the velocity vector, p the pressure, μ the dynamic viscosity, and $\mathbf{f}$ a volumetric force vector. The interface Γ_i between the fluid and solid regions is defined using a level-set function ψ which is defined as a signed distance function from the immersed interface:

$$\psi(\mathbf{x}) = \begin{cases} d(\mathbf{x}, \mathbf{x_i}), & \mathbf{x} \text{ in the fluid region,} \\ 0, & \mathbf{x} \text{ on the fluid/solid interface,} \\ -d(\mathbf{x}, \mathbf{x_i}), & \mathbf{x} \text{ in the solid region,} \end{cases} \quad (3)$$

where $d(\mathbf{x}, \mathbf{x_i})$ is the distance between the point $P(\mathbf{x})$ and the fluid/solid interface. Hence, points in the fluid region will take on positive values of ψ, whereas ψ will be negative for points in the solid region.

The boundary conditions associated to the momentum-continuity equations are

$$\mathbf{u} = \mathbf{U}_D(\mathbf{x}), \qquad \text{for } \mathbf{x} \in \Gamma_D, \quad (4)$$

$$\mu \left(\nabla \mathbf{u} + \nabla \mathbf{u}^T \right) \cdot \hat{\mathbf{n}} - p\hat{\mathbf{n}} = \mathbf{t}(\mathbf{x}), \qquad \text{for } \mathbf{x} \in \Gamma_t, \quad (5)$$

where Γ_D is the portion of the fluid boundary $\partial\Omega_f$ where Dirichlet conditions are imposed, and $\mathbf{t}$ is the traction imposed on the remaining fluid boundary $\Gamma_t = \partial\Omega_f \backslash \Gamma_D$. Dirichlet boundary conditions are imposed at the interface between fluid and solid regions. Because this interface is not represented by the finite element discretization, a special procedure is used to enforce velocity boundary conditions on this surface. This approach is described in details in reference [1].

Solution algorithm

The numerical solutions are obtained using a multi-scale approach. In a first study, the 3D Navier-Stokes equations describing the fluid flow at pore level are solved. For this, the level set function representing the metallic foam surface (solid boundary) is constructed using micro-CT scan reconstructions. The resulting surface information is used within a finite element immersed boundary method to solve the flow inside the metallic foam. The micro scale solution of the flow takes into account the details characterizing the geometry of the foam and is used to determine the permeability coefficients in the Forchheimer's model. In a second step, a numerical approach is used to solve the flow at the macro scale, (in this case the scale of the experimental apparatus), by modelling the presence of the foam via a source term providing the same pressure drop as the one computed at the micro scale. Such a simulation gives the opportunity to solve the flow in complex configurations in which the foam is only a part of the computational domain.

The immersed boundary method

The flow equations were solved using a finite element method coupled with an immersed boundary approach [1]. In the present work, the entire domain including fluid and solid regions were discretized. A special treatment was applied when solving for nodes in the solid region. The mesh was intersected by the fluid/solid interface at points located along element edges. Those points were considered as additional degrees of freedom in the finite element formulation. The fluid/solid interface was defined by a level-set function and the additional nodes were determined as those for which $\psi = 0$. Moreover, because the level-set function is interpolated using linear shape functions, the intersection between the interface and a tetrahedral element is a plane, either a triangle or a quadrilateral. Elements cut by the interface are therefore decomposed into sub-elements which are either entirely in the fluid or entirely in the solid regions. The addition of degrees of freedom associated to the nodes on the interface would normally result in a modification of the global matrix resulting from the finite element equations. In such a case, the implementation is more challenging and the increase in computational cost is inherent as dynamic data structures and renumbering are needed. The present approach does not need the explicit addition of the degrees of freedom associated to those nodes. The procedure is described in details in reference [1].

Imposition of prescribed pressure drop

The permeability of the metallic foam was obtained using the Forchheimer's equation representing an empirical relationship between the pressure drop Δp and the mean flow rate u_0:

$$\frac{\Delta p}{L} = \frac{\mu}{k_1} u_0 + \frac{\rho}{k_2} u_0^2 \quad (6)$$

where k_1 and k_2 are model coefficients. In dimensionless form the Forchheimer's equation is written as follows:

$$\frac{\Delta \tilde{p}}{\tilde{L}} = \frac{1}{Re} \frac{1}{\tilde{k}_1} + \frac{1}{\tilde{k}_2} \quad (7)$$

with $\tilde{k}_1 = k_1 / L_0^2$ and $\tilde{k}_2 = k_2 / L_0$.

Finite element solution

The incompressible Navier-Stokes equations are solved by a SUPG formulation [2, 3]. The SUPG method contains additional stabilization terms which are integrated only on the element interiors. These terms provide smooth solutions to convection dominated flows and deal with the velocity-pressure coupling so that equal-order interpolation results in a stable numerical scheme [2]. This makes possible the use of elements that do not satisfy the Babuška-Brezzi condition as is the case of the linear $P1-P1$ element [4]. SUPG also stabilizes the resulting linear systems, making them amenable for robust iterative solution. This last advantage is of critical importance for large scale applications. For the Navier-Stokes equations and the linear elements used here SUPG and GLS methods are identical.

The nonlinear equations for the velocity and pressure were solved with a few Picard steps followed by Newton-Raphson iterations. The resulting linear systems were generated directly in a compressed sparse row format, and solved using the bi-conjugate gradient stabilized (Bi-CGSTAB) iterative method with an ILU preconditioner. An important reason for using the SUPG formulation is that it also stabilizes the linear systems, making them tractable by iterative solvers.

VALIDATION: FLOW AROUND AN ARRAY OF SPHERES

The IB method was first verified on a test problem corresponding to the flow around spheres placed on a simple cubic lattice. A non-dimensional solution was obtained by defining reference values for the variables describing both the immersed geometry and the flow. The reference length was taken equal to the distance between the center of adjacent spheres L and the reference velocity was given by the inlet velocity V_i. Following the work of Martys *et al.* [5] computations were carried out without considering the inertia in the momentum equations (low Reynolds number approach). The dimensionless viscosity and inlet velocity were set to 1 and the dimesionless diameter of the spheres $\tilde{D} = D/L$ was varied between 0.2 and 1.4, resulting in the solid fraction of the bed of spheres varying from $4.19 \cdot 10^{-3}$ to 0.959.

Given the symmetry of the arrangement of spheres, only one array having the size of the transverse section equal to the distance between the centroids of two adjacent spheres were considered. Computations were carried out for 5 and respectively 9 spheres in the flow direction. The surface of the spheres on which Dirichlet boundary conditions should be imposed is represented

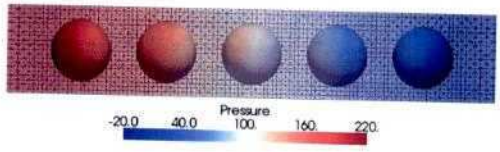

FIGURE 1. Pressure distribution and computational mesh.

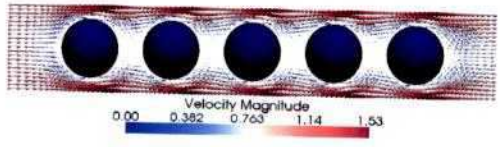

FIGURE 2. Flow field around the spheres.

by the level-set function:

$$\psi(x,y,z) = min(\psi_0, \left((x-x_i)^2 + (y-y_i)^2 + (z-z_i)^2\right)^{1/2} - D/2), \text{ for } i = 1, N_s \quad (8)$$

where N_s is the number of spheres in the array, ψ_0 is an arbitrary positive value larger than the size of the computational domain (say $\psi_0 = 100$) and (x_i, y_i, z_i) are the centroid coordinates of the sphere i. The level-set $\psi = 0$ will then indicate the location of the boundary. The region having $\psi > 0$ is the flow region inside which the flow equations were solved and the region having $\psi < 0$ represents the volume of the spheres. The solid fraction of the bed of spheres for a given sphere radius $R = D/2$ is given by:

$$f_s = V_s / V_{tot} \quad (9)$$

where V_s is the volume of one sphere and $V_{tot} = L^3$ is the volume of the cubic box of size L within which the sphere is located. In dimensionless variables ($L = 1$) the volume of the box is equal to unity and the volume of the sphere is given by:

$$V_s = \frac{4\pi R^3}{3}, \quad \text{for } R \leq 0.5 \quad (10)$$

$$V_s = \frac{4\pi R^3}{3} - 4\pi R^3 + \frac{\pi L}{4}\left(12R^2 - L^2\right), \text{ for } R > 0.5 \quad (11)$$

The expression in equation (11) takes into account the overlapping of the spheres when $R > 0.5$.

The solution for the pressure distribution on the surface of the spheres is shown in Figure 1 for an array of 5 spheres of diameter 0.7. The pressure distribution and the mesh are also shown in a mid-plane along the flow direction. The mesh has 20 elements in directions transverse to the flow. The solid boundary of the spheres cuts through the elements, as the mesh is not constructed to fit the geometry of the immersed objects. The flow field for

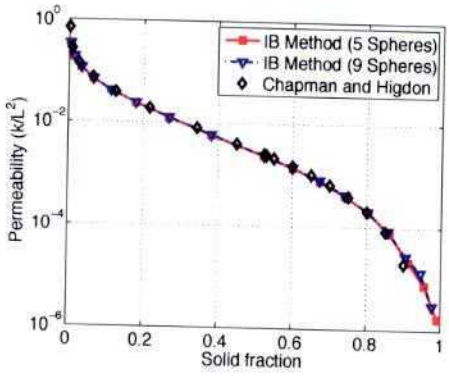

FIGURE 3. Permeability of an array of spheres.

the same case is presented in Figure 2 in the plane containing the centers of the spheres, indicating that homogeneous velocities are recovered on the sphere surface.

Hereafter we present the results obtained for the pressure drop in the flow and the resulting permeability coefficient for various diameters of the spheres. The permeability k of the array of spheres is determined from the Darcy's law and is given by:

$$k = \frac{\mu \overline{u}}{|\nabla p|} \tag{12}$$

where $\overline{u}$ is the average flow rate.

The solution for the permeability of the array of spheres is shown in Figure 3 as a function of the solid fraction. The results obtained by Chapman and Higdon [6] are also presented as a reference. Similar results were reported by Martys *et al.* [5] using a lattice Boltzmann method. As can be seen, the permeability decreases as the solid fraction increases, reaching a value close to zero when the solid fraction approaches the maximum value of 1. The present numerical results agree very well with those reported by Chapman and Higdon [6].

APPLICATION: FLOW THROUGH A METALLIC FOAM MATRIX

The present test problem is the flow of water through a metallic foam. The foam is an open cell nickel chromium foam from Recemat (NC-1723) having average pore size of 0.9mm as shown in Figure 4. Experimental measurements were reported by Innocentini *et al.* [7] for the flow through various thicknesses of the foam, ranging from 4.3mm to 38.6mm. The setup is illustrated in Figure 5. The ratio between the surface of the nominal flow section to the surface of the sample is 0.87.

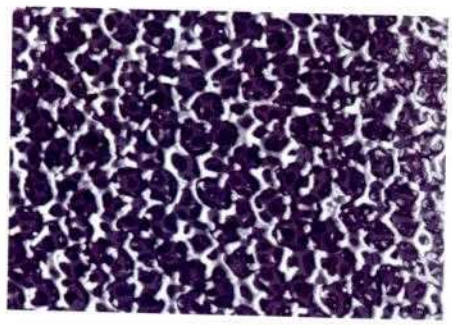

FIGURE 4. Metallic foam used for this study.

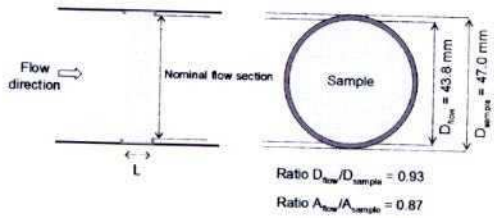

FIGURE 5. Details of the experimental setup.

Micro-scale simulations

For the micro-scale simulations the metallic foam surface of a small sample having 3.03mm x 3.03mm x 4.04mm is determined using micro-CT scan reconstructions. The scan has a resolution of 0.0101mm, thus providing data at 300 x 300 x 400 points. This information is then used to initialize the level-set function representing the surface of the metallic foam. The water density and viscosity are taken as $\rho = 996.1 kg/m^3$ and $\mu = 8.3 \cdot 10^{-4} Pa \cdot s$.

Three series of simulations were carried out: (case 1) for the flow in the z-direction, (case 2) for the flow in the x-direction, and (case 3) for the flow in the x-direction in a sample having twice the length of the original sample ($6.06mm$ instead of $3.03mm$). The computational domain for each case extends 2mm before the foam sample and 20mm in the wake.The mesh is uniform in the region covering the foam and has either 60x60x80 nodes or 75x75x100 nodes. The pressure distribution for the case 1 at a velocity of $0.308m/s$ and the finner mesh is shown in Figure 6, whereas the velocity vectors in a cross-section along the flow direction are plotted in Figure 7. The pressure decreases in the direction of the flow. Regions of higher pressure are observed where the flow impacts the foam walls and lower pressure is obtained in the wake behind the foam structure. Figure 7 indicates that the flow accelerates in the sections which are not filled by the foam material and several recirculation regions are observed behind the foam structure.

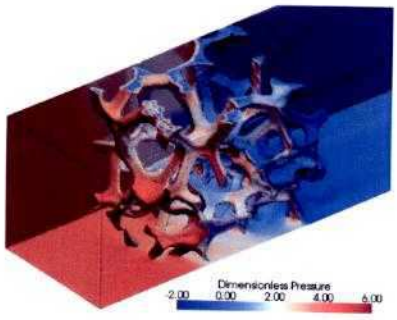

FIGURE 6. Pressure distribution for case 1.

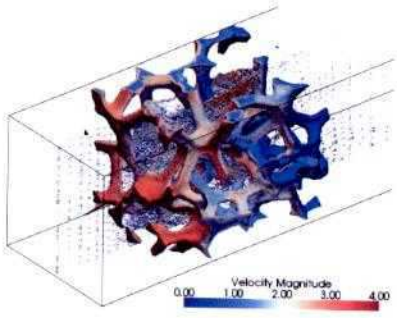

FIGURE 7. Velocity vectors for case 1.

The pressure gradient in the flow direction was computed as a function of the inlet velocity. First, the case 1 was computed for the two mesh sizes in order to determine the dependence of the solution on the mesh. Including the regions before and after the foam, the two meshes have 1,872,000 elements, 390,705 nodes for the 60x60x80 mesh and respectively 3,487,500 elements and 722,000 nodes for the 75x75x100 mesh. As can be seen from Figure 8, the solution depends very little on the mesh size for this level of refinement.

The effect of the size of the sample was verified by comparing the cases 2 and 3. In both cases the flow was in the x-direction and simulations for case 3 were carried out on a sample twice as long as the one for the case 2. The size of the sample is shown to have little effect on the pressure gradient in the foam (see Figure 9). This is an indication that the size of the sample is representative for computing the permeability of the foam.

The numerical results from cases 1, 2 and 3 were used to compute the coefficients k_1 and k_2 in the Forchheimer's equation. The results were compared with those obtained experimentally and good agreement with the computed pressure gradients is obtained for $k_1 = 2.16 \cdot 10^{-8} m^2$ and $k_2 = 9.5 \cdot 10^{-4} m$ [8]. The pressure gradient given by the Forchheimer's equation is compared with the computed pressure gradient in Figure 9.

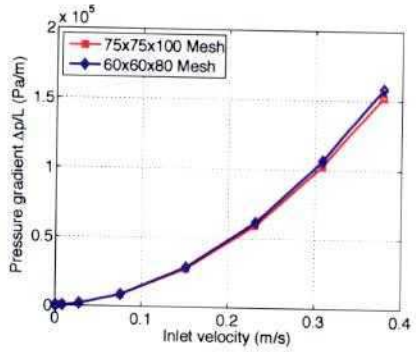

FIGURE 8. Influence of the mesh size for case 1.

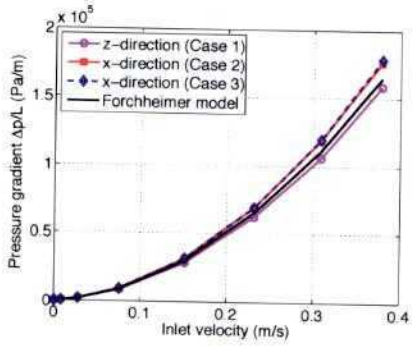

FIGURE 9. Forchheimer model data vs computed solutions.

Macro-scale simulations

The micro scale simulations provide the pressure drop as a function of the flow rate and hence the permeability coefficients of the foam (the coefficients used in the Forchheimer's equation). This information is then used to perform macro-scale simulations describing the experimental setup shown in Figure 5. The solution was computed on a cylindrical domain having $47mm$ in diameter, a length of $282mm$ upward from the foam location and $200mm$ downward from the foam. As in the experiment, the foam thickness were $4.27mm$, $8.6mm$, $13.7mm$, $21.0mm$, $28.2mm$, and $38.6mm$. The pressure and velocity in a plane through the symmetry axis are shown in Figures 10 and 11 respectively, for the case $L = 38.6mm$ and an inlet velocity of $0.305m/s$.

The pressure drop determined by the presence of the

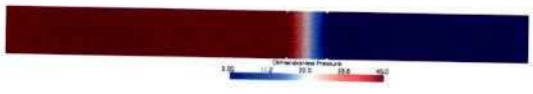

FIGURE 10. Pressure distribution for $L = 38.6mm$.

FIGURE 11. Velocity distribution for $L = 38.6mm$.

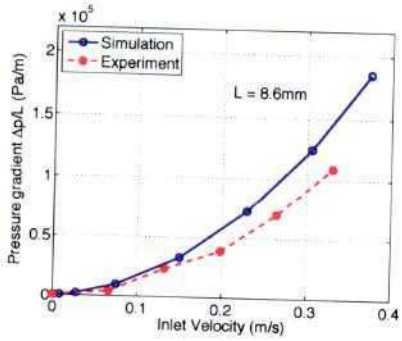

FIGURE 12. Pressure gradients for $L = 8.6mm$.

foam was calculated between two locations at $50mm$ on each side of the foam. The numerical results are compared with the experimental data in Figure 12 for $L = 8.6mm$ and in Figure 13 for $L = 38.6mm$. As can be seen, the agreement between the simulation and experiment improves when increasing the thickness of the foam. Figure 14 indicates that the pressure gradient sensitivity to the foam thickness is small for this experimental setup.

CONCLUSION

This work presents a multi-scale methodology for characterizing numerically the flow permeability through porous medium. The approach was validated with an open cell metallic foam. The proposed approach considers both the foam details at the pore level and the actual behavior when placed inside more complex flow configurations. Simulation results agree very well with the experimental data, thus opening the way for more extensive numerical studies of the flow inside complex porous medium. Such approach could be used for the design and optimization of new devices involving flow through porous materials.

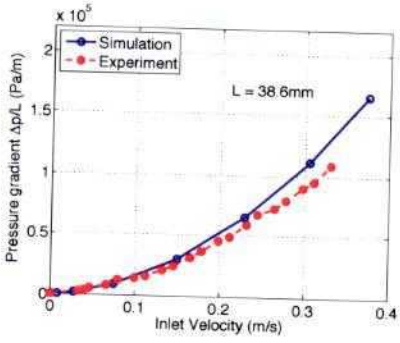

FIGURE 13. Pressure gradients for $L = 38.6mm$.

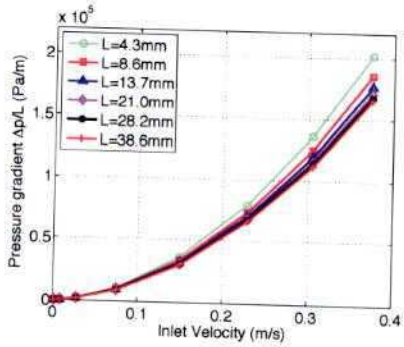

FIGURE 14. Solutions for different foam thickness.

REFERENCES

1. F. Ilinca and J.-F. Hétu, "A finite element immersed boundary method for fluid flow around rigid objects," *Int. J. Num. Methods Fluids*, published online, 2010.
2. L.P. Franca and S.L. Frey, "Stabilized finite element methods: II. The incompressible Navier-Stokes equations," *Comp. Methods Appl. Mech. Engng.*, vol. 99(2-3), pp. 209–233, 1992.
3. F. Ilinca, J.-F. Hétu, and D. Pelletier, "On stabilized finite element formulations for incompressible advective-diffusive transport and fluid flow problems," *Comp. Methods Appl. Mech. Engng.*, vol. 188, pp. 235–255, 2000.
4. T. J. R. Hughes, L. P. Franca, and M. Balestra, "A new finite element formulation for computational fluid dynamics: V. Circumventing the Babuška-Brezzi condition: A stable Petrov-Galerkin formulation of the Stokes problem accommodating equal-order interpolations," *Comp. Methods Appl. Mech. Engng.*, vol. 59, pp. 85–99, 1986.
5. N.S. Martys, J.G. Hagedorn, D. Goujon, and J.E. Devaney, "Large Scale Simulations of Single and Multi-Component Flow in Porous Media," Proc. SPIE Conference on Developments in X-Ray Tomography II, *SPIE*, vol. 3772, pp. 205-213, 1999.
6. A.M. Chapman and J.J.L. Higdon, "Oscillatory Stokes flow in periodic porous media," *Phys. Fluids A*, vol. 4, pp. 2099–2116, 1992.
7. M.D.M. Innocentini, L.P. Lefebvre, R.V. Meloni and E. Baril, "Influence of sample thickness and measurement set-up on the experimental evaluation of permeability of metallic foams," in press in *J. of Porous Materials*, 2010.
8. J.P.Bonnet, F.Topin, L.Tadrist, "Flow Laws in Metal Foams: Compressibility and Pore Size Effects," *Transp. Porous Med.*, vol. 73, no. 2, pp.233-254, 2008.